Formation and Sustainment of Field-reversed Configuration by Rotating Magnetic Field with Spatial High-harmonic Components

M. Inomoto[1] 1), K. Yambe 1), K. Kitano 1), S. Okada 1)

1) Center for Atomic and Molecular Technologies, Osaka University, Osaka, Japan

e-mail contact of main author: inomoto@k.u-tokyo.ac.jp

Abstract. Field-reversed configurations (FRCs) sustained by rotating magnetic fields (RMFs) with spatial high-harmonic components have been studied in the metal flux conserver of the FRC injection experiment (FIX) apparatus. The high-harmonic RMF method has some unique features; (1) field lines of the RMF do not penetrate or cross the vessel wall, (2) selective penetration/exclusion of the fundamental/high harmonic RMF component will result in a generation of effective magnetic pressure near the separatrix, which helps to keep the separatrix away from the vessel wall, (3) strong azimuthal non-uniformity of the RMF will bring about the $n = 4$ deformation of the core FRC plasma, which will suppress the destructive modes caused by the rotation of the plasma column. The RMF with spatial high-harmonic components will provide quasi-steady current drive of high-beta FRC plasmas without destructive $n = 2$ rotational mode and will be helpful in reducing the particle loss and thermal load when applied to the fusion core plasma.

1. Introduction

A field-reversed configuration (FRC) [1] is a compact toroidal plasma with extremely high beta value close to unity. It is attractive as a core plasma for advanced fuel (i.e. D-^{3}He) nuclear fusion [2]. Field-reversed theta pinch (FRTP) method [3] has been employed for a long time as a prevalent technique to form an FRC with high density and temperature; however, it involves a crucial defect of a short discharge duration due to the absence of efficient current drive or additional heating methods. It has been a major issue in FRC experimental researches to extend discharge period and confinement times. Novel formation techniques using merging spheromak plasmas [4-6] and rotating magnetic field (RMF) [7-12] were recently suggested and intensively studied. The RMF is one of the most successful current-drive methods for high-beta and singly-connected FRC plasmas since it is capable of driving non-inductive plasma current without external coils intersecting the plasma. Quasi-steady sustainment of FRC plasmas with reasonably high plasma temperature has been established by using a symmetric dipole RMF [9], which consists only of the azimuthal mode component of $n = 1$; however, simple dipole RMF is liable to open up the FRC's closed surfaces and to degrade the energy and particle confinement. In order to resolve this problem, a RMF method using spatial high-harmonic components [11,12] has been proposed and experimentally investigated in the FRC injection experiment (FIX) in which the RMF antennas are located inside a conducting vacuum vessel (see FIG. 3).

This new method brings about some unique features on RMF-FRC equilibrium. First of all, the field lines of the RMF do not penetrate or cross the vessel wall. This will bring about improvement of the energy and particle transport properties. Another important feature is that the rotation frequency of the spatial high-harmonic components is slower and sometimes in the reverse direction compared to the fundamental component of the RMF. Thus the fundamental $n = 1$ component of the RMF is expected to penetrate into the plasma, while the high-harmonic components are excluded at the plasma edge. This selective

---

[1] Present address : Graduate School for Frontier Sciences, The University of Tokyo, Chiba, Japan

penetration/exclusion results in a generation of effective magnetic pressure near the separatrix, which helps to keep the separatrix away from the vessel wall.

The other feature is that the strong azimuthal non-uniformity of the RMF brings about the $n = 4$ deformation of the quasi-steady core FRC, which will, together with the radially increasing nature of the confining magnetic field pressure, suppress the destructive modes driven by the rotation of the plasma column [13,14].

2. Rotating Magnetic Field with High-harmonic Components

The temporary oscillating variables $\tilde{X}$ resulting from the two-phase RMF will be expressed as

$$\tilde{X} = \sum_n X_n \cos n\theta \sin\omega t + \sum_n X_n \cos n(\theta - \pi/2)\sin(\omega t - \pi/2), \qquad n = 1, 3, 5, \cdots$$

$$= X_1 e^{i(\omega t - \theta)} + X_3 e^{i(\omega t + 3\theta)} + X_5 e^{i(\omega t - 5\theta)} + X_7 e^{i(\omega t + 7\theta)} + \cdots \tag{1}$$

The spatial high-harmonic components with mode $n = 2k - 1 (k = 1, 2, 3, \cdots)$ rotate with the angular frequency of $\pm \omega/n$, where the sign is positive for odd k number (or $n = 1, 5, 9, \cdots$) and negative for even k number (or $n = 3, 7, 11, \cdots$). The high-harmonic components then have slower or reversed rotation frequency compared with the fundamental $n = 1$ component. The vacuum RMF lines of force calculated on the assumption that the chamber wall is a perfect conductor is shown in FIG. 1(a). The vacuum RMF is rather straight near the geometric axis, i.e. the fundamental $n = 1$ component is dominant. The spatial high-harmonic components with odd azimuthal mode numbers of $n = 3, 5, 7,\ldots$ become significant in the vicinity of the antenna
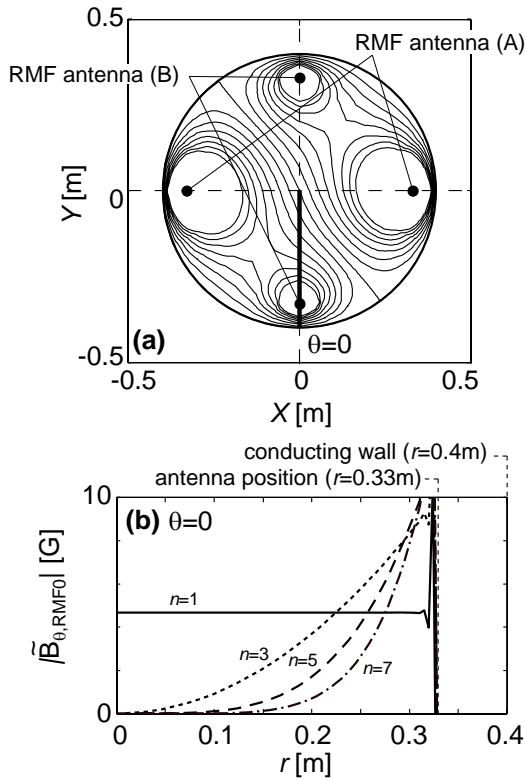

FIG. 1. (a) 2-dimensional field line structure and (b) the radial profile of the vacuum RMF inside a conducting vessel at $\theta = 0$.
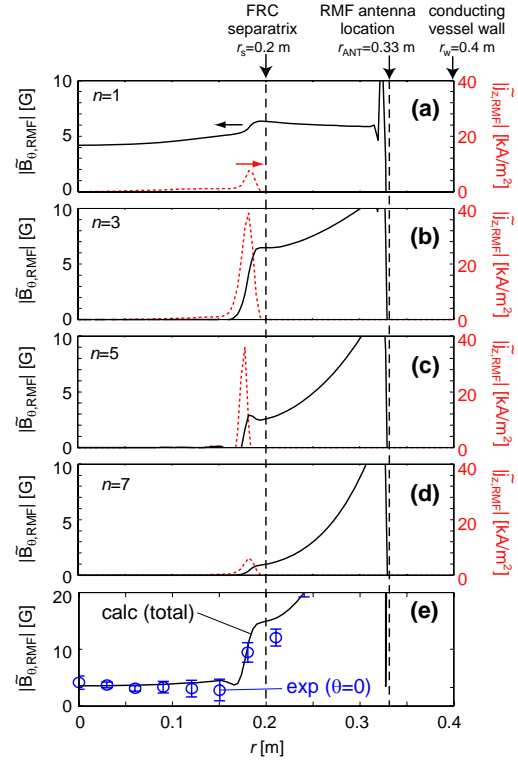

FIG.2. Radial profiles of (a-d) the oscillating magnetic field and the shielding current density in the calculated 1-dimensional RMF-FRC equilibrium, and (e) the experimentally observed oscillating magnetic field profile.

position partly because of the image current flowing on the conducting vessel. The radial profile of the vacuum RMF $\left|\tilde{B}_{\theta,RMF0}\right|$ at the azimuthal position θ = 0 where the RMF antenna exists is shown in FIG. 1(b). The fundamental n = 1 component is uniform inside the antenna position, and the high-harmonic components rise at outer radial position. Since the high-harmonic components are expected to be excluded almost completely from the plasma region, they will exert magnetic pressure in such a way as to prevent the separatrix radius from being much larger than the position where the high-harmonic components of the vacuum RMF become dominant (r ~ 0.2m). At the azimuthal position θ = π/4 (between antennas) the amplitude of the vacuum RMF $\left|\tilde{B}_{\theta,RMF0}\right|$ is same as the case at θ = 0, but the phase of n = 3, 5, 11, 13,… are inverted.

The 1-dimensional FRC equilibrium sustained by the RMF satisfies both the radial and azimuthal force balances. The radial pressure balance equation is written as follows, assuming axial uniformity, uniform temperatures and the immobile ions,

$$j_\theta B_z - \left\langle \tilde{\tilde{j}}_{z,RMF}\tilde{B}_{\theta,RMF} \right\rangle = \frac{\partial p}{\partial r} \approx k(T_i + T_e)\frac{\partial n_e}{\partial r}, \qquad (2)$$

where $j_\theta = -en_e\omega_e r$, ω_e is the electron rotation frequency, $\tilde{\tilde{j}}_{z,RMF} = -(1/\mu_0)\nabla^2\tilde{A}_z$, $\tilde{B}_{\theta,RMF} = -\partial\tilde{A}_{z,RMF}/\partial r$ and the bracket $\langle\ \rangle$ represents average over an RMF cycle. In the azimuthal direction, the RMF torque on plasma electrons $f_{\theta,RMF}$ will balance the collisional drag force $f_{\theta,coll} = \nu\, m_e n_e \omega_e r$ due to the electron-ion and electron-neutral collisions. The azimuthal balance equation is written as

$$\nu\, m_e n_e \omega_e r = \left\langle \tilde{\tilde{j}}_{z,RMF}\tilde{B}_{r,RMF} \right\rangle, \qquad (3)$$

where ν is the electron collision frequency and $\tilde{B}_{r,RMF} = (1/r)\partial\tilde{A}_{z,RMF}/\partial\theta$. The RMF-FRC equilibrium will be represented using these radial and azimuthal balance equations with the oscillating RMF components of $\tilde{\tilde{j}}_{z,RMF}$, $\tilde{A}_{z,RMF}$ and the steady FRC quantities such as j_θ, B_z, n_e and ω_e.

The screening current $\tilde{\tilde{j}}_{z,RMF}$ flowing in the plasma is expressed as

$$\tilde{\tilde{j}}_{z,RMF} = \frac{1}{\eta_{//}^*}\left(\tilde{E}_{z,RMF} - \omega_e r\tilde{B}_{r,RMF}\right) = -\frac{1}{\eta_{//}^*}\left(i\omega + \omega_e\frac{\partial}{\partial\theta}\right)\tilde{A}_{z,RMF}, \qquad (4)$$

where $\eta_{//}^* = \eta_{//} + i\omega\left(m_e/e^2 n_e\right)$ is the effective resistivity and $\eta_{//}$ is the parallel classical resistivity. The system of equations (2)(3)(4) yields RMF-FRC equilibrium and will be solved numerically using an iterative method. If the FRC's steady quantities such as axial magnetic field, azimuthal current density and electron density are assumed to be uniform in the azimuthal direction, in other words, they consist only of the n = 0 components, the oscillating RMF quantities appear in the equations (2)(3)(4) can be decomposed to each Fourier component and the system is handled as 1-dimensional equilibrium expressed by a linear summation of each azimuthal mode [11].

The radial profiles of the RMF in the presence of the FRC plasma are calculated using this simple 1-dimensional RMF-FRC equilibrium model and shown in FIG. 2(a-d) together with

the profiles of the shielding current density flowing in the axial direction. The high-harmonic components, particularly the modes of $n = 3$ and 5, are excluded at the plasma edge and provide a large $\langle j_z B_\theta \rangle$ inward force on the plasma edge. Though the fundamental $n = 1$ component is partly shielded at the plasma edge, it reaches to the geometric axis to supply the azimuthal torque on the entire plasma column. FIG. 2 (e) shows the radial profile of the RMF $\left| B_{\theta,RMF} \right|$ measured by the magnetic probe array (circle symbols). The experimental result shows that large part of the RMF is screened near the plasma edge ($r \sim 0.2$ m), although certain magnitude of the RMF reaches the plasma center. These experimental results agree well with the numerical model qualitatively.

3. Experimental Setup

The RMF antennas are located at $r_{ANT} = 0.33$ m inside a conducting vacuum vessel wall of the FIX confinement section located at $r_w = 0.4$ m. The Schematic cross-sectional view of the FIX confinement section is show in FIG. 3. Two pairs of RMF antennas are energized by two independent forward-type inverter circuits with the phase difference of π/2. Typical RMF angular frequency is $\omega = 670 \times 10^3$ rad/s and RMF current is 800 A. Highly ionized plasma generated by a washer gun is injected into the central region of the device, where the RMF is already applied. After the initial unstable period, the RMF begins to drive current, forming an FRC with closed magnetic field lines. Even though the typical electron density $n_e = 5 \times 10^{17}$ m^{-3} and temperature $T_e = 3$ eV are much smaller than those in the existing FRC experiments, the RMF-FRC holds the radial pressure balance, high-beta nature, and rigid-rotor-like current and density profiles.

Internal magnetic probe arrays are used to measure both radial and axial profiles of the steady axial magnetic field. The radial probe arrays are located at two different azimuthal locations of θ = 0 and π/4 and each of them consists of 13 pick-up coils with radial spacings of 30 mm. The electron density is measured by a movable Langmuir probe located at θ = π/4.

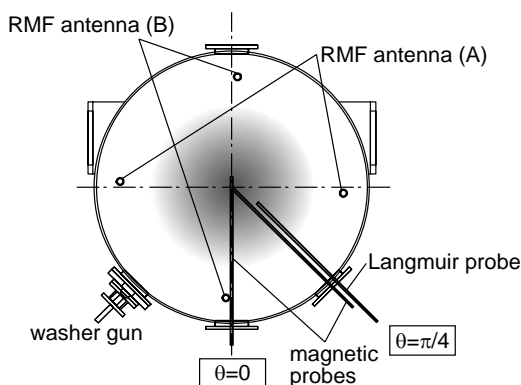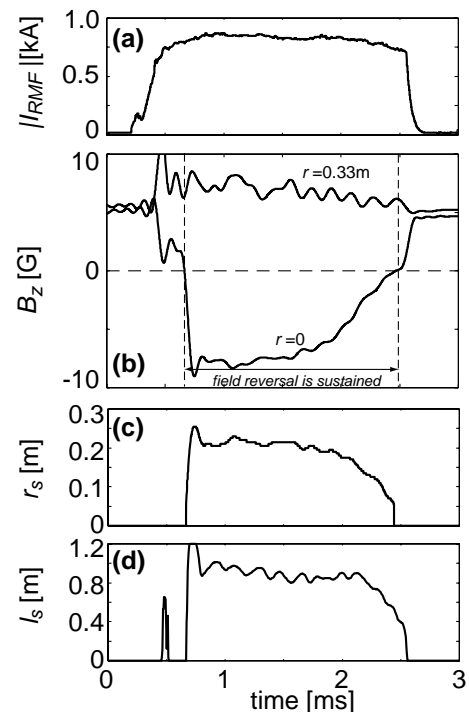Fig. 4. Time evolutions of (a) RMF antenna current, (b) axial magnetic field, (c) separatrix radius and (d) separatrix length.

FIG. 3. Cross-sectional view of the FRC injection experiment (FIX) apparatus.

4. Experimental Results and Discussions

FIG. 4 shows the time evolutions of the RMF antenna current, axial magnetic fields, separatrix radius and separatrix length measured on the midplane at $z = 0$ and $\theta = 0$. The axial magnetic field inside the plasma shows large reversal for about 1.5 ms-duration, which corresponds to ~100 Alfvèn transit time. The global stability might be provided by the kinetic effect since the ion collisionless skin depth is even larger than the separatrix radius. The separatrix radius r_s is about 0.2 m, or $x_s = r_s / r_w \sim 0.5$ during the flat top phase. This value is much smaller than those observed in previous results from purely dipole RMF [7-9]. The separatrix length l_s during the flat top phase is about 0.8 m, keeping moderate elongation of about 2.

The radial profiles of the axial magnetic field measured at $\theta = 0$ is shown in FIG. 5(a). The experimental results indicated by triangle markers show good agreement with values which are predicted by a purely radial 1-dimensional RMF-FRC equilibrium model [11] calculated at $\theta = 0$. The numerical RMF-FRC equilibrium has steep density and current gradients near the separatrix, as shown in FIG. 5(b). This gradient is mainly sustained by the effective magnetic pressure of the excluded high-harmonic components of the RMF. FIG. 5(c) shows the radial profile of radial Lorentz force $j_\theta B_z$ of the steady FRC and the ponderamotive force $\langle \tilde{j}_{z,RMF} \tilde{B}_{\theta,RMF} \rangle$ from the oscillating RMF. The high-harmonic components of the RMF are screened near the plasma edge and generate a large ponderamotive force localized at the edge region. This pondramotive force plays a dominant role on keeping the plasma separatrix away from the wall.

On the other hand, the RMF-FRC equilibrium at $\theta = \pi/4$ shows a quite different feature. Because of the strong azimuthal non-uniformity of the oscillating RMF, the equilibrium of the steady FRC is expected to have azimuthal deformation of $n = 4, 8,\dots$. The amplitude of the RMF is much smaller at $\theta = \pi/4$, where the RMF antenna is absent, than that at $\theta = 0$ just
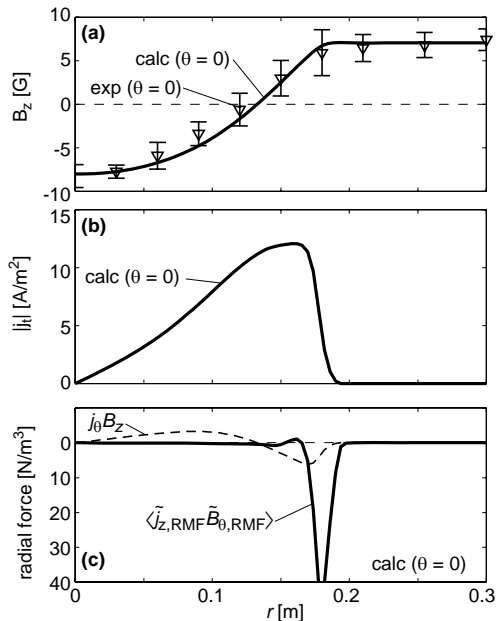

FIG.5. Radial profiles of (a) axial magnetic field, (b) azimuthal current density and (c) radial force at $\theta = 0$.
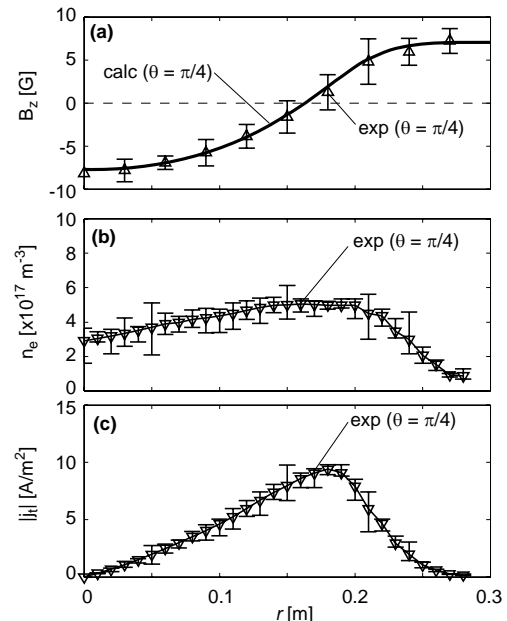
FIG.6. Radial profiles of (a) axial magnetic field, (b) electron density and (c) azimuthal current density at $\theta = \pi/4$.

inside the antenna ($r_{ANT} = 0.33$ m). FIG. 6(a) shows the radial profiles of axial magnetic field measured at $\theta = \pi/4$. The FRC plasma has much broader magnetic field profile at $\theta = \pi/4$,
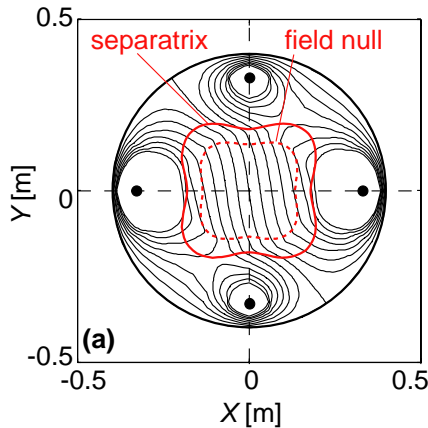

FIG.7. 2-dimensional field line structure of the RMF with n = 4 deformed FRC.

indicating that the plasma current driven by the RMF is not a simple circular current but has azimuthal structure. The radii of the separatrix r_s is about 0.2 m at $\theta = 0$ and about 0.24 m at $\theta = \pi/4$. FIG. 6(b) and (c) show the radial profiles of the electron density n_e and the azimuthal current density j_t which is defined as a product of the measured electron density and the electron rotation frequency. As the FRC extends radially outward at this azimuthal location, the azimuthal current flows rather outboard side of the configuration, providing enough Lorentz force $j_\theta B_z$ to confine the plasma pressure without large contribution from the equivalent magnetic pressure of the excluded RMF [12]. FIG. 7 shows the 2-dimensinoal structure of the RMF lines of force calculated for the RMF-FRC equilibrium with $n = 4$ deformation. The plasma shape, or the plasma current flow pattern, looks more like a square with rounded corners.

The FRC sustained by the high-harmonic RMF rarely exhibited density oscillation due to the rotational instability which is commonly observed in the FRC plasma produced by the field-reversed theta pinch method [13,14]. The azimuthal deformation of the FRC plasma sustained by the RMF with high-harmonic components might be providing essential stabilization against the destructive modes by decreasing the rotation of the plasma column in a similar manner as the multipole field [15,16]. The stability criterion for the rotational mode by $n = 4$ multipole field is given by

$$B_s \geq \left(r_s \mid \Omega \mid / 2\right)\sqrt{\mu_0 \rho} \tag{5}$$

using the 2-dimensinal ideal MHD approximation [16], where B_s is the vacuum multipole field at $r = r_s$, Ω is the rotation angular frequency of the plasma column and ρ is the mass density. If the ions were assumed to be rotating synchronously with the RMF field, then the criterion to stabilize the rotational mode becomes as $B_s \geq 20$ G from equation (5). This value is considerably larger than the actual multipole field amplitude shown in FIG. 1(b). In reality, the ions in the RMF-FRC equilibrium are not considered to be accelerated that much due to the drug by neutral particles [17].

In order to evaluate a reasonable stabilization mechanism, development of realistic 2-dimensional RMF-FRC equilibrium is required. In the simple 1-dimensional model, the oscillating RMF components are expressed as a linear summation of the odd azimuthal mode numbers of $n = 1, 3, 5, 7,\dots$However, when the steady FRC quantities of ω_e and $\eta_{//}^*$ have the azimuthal deformation such as $n = 4, 8,\dots$, each azimuthal mode of the RMF quantities of $\tilde{j}_{z,RMF}$ and $\tilde{A}_{z,RMF}$ will be nonlinearly coupled through the equation (4). As a consequence, the simple 1-dimensional model is NOT appropriate to achieve a self-consistent 2-dimensional RMF-FRC equilibrium with azimuthal deformation of the steady FRC quantities.

5. Summary and Conclusions

The properties of the FRC sustained by the RMF with spatial high-harmonic components are studied numerically and experimentally. The RMF with high-harmonic components has different penetration properties from the simple dipole RMF, resulting in a generation of effective magnetic pressure near the separatrix. This feature helps to keep the separatrix away from the vessel wall. The azimuthal deformation of the FRC plasma due to the strong non-uniformity of the RMF will provide stabilization against the destructive modes by decreasing the rotation of the plasma column, although further numerical study involving nonlinear coupling of RMF modes is required to evaluate the self-consistent RMF-FRC equilibrium. The proposed RMF method will provide quasi-steady current drive of high-beta FRC plasmas with essential stabilization against destructive $n = 2$ rotational mode and will be helpful in reducing the particle loss and thermal load when applied to the fusion core plasma.

Acknowledgements

References
[1] M. Tuszewski, Nucl. Fusion **28**, 2033 (1988).
[2] H. Momota et al, Fusion Tech **21**, 2307 (1992).
[3] W.T. Armstrong et al, Phys. Fluids **24**, 2068 (1981).
[4] Y. Ono et al, Nucl. Fusion **39**, 2001 (1999)
[5] C.D. Cothran et al, Phys. Plasmas **10**, 1748 (2003).
[6] S.P. Gerhardt et al, Phys. Rev. Lett. **99**, 245003 (2007).
[7] I.R. Jones, Phys. Plasmas **6**, 1950 (1999).
[8] J.T. Slough and K.E. Miller, Phys. Plasmas **7** ,1945 (2000).
[9] H.Y. Guo et al., Phys. Plasmas 15, 056001 (2008).
[10] S. Cohen et al, Phys. Rev. Lett. **98**, 145002 (2007).
[11] M. Inomoto et al., Phys. Rev. Lett. **99**, 175003 (2007).
[12] K. Yambe et al., *"Effects of internal structure on equilibrium of field-reversed configuration plasma sustained by rotating magnetic field"*, Phys. Plasmas **15**, to be published .
[13] T. Asai et al., Phys. Plasmas **13**, 072508 (2006).
[14] L. Steinhauer, Phys. Plasmas **15**, 012505, (2008).
[15] S. Ohi, et al., Phys. Rev. Lett. **51**, 1042 (1983).
[16] T. Ishimura, Phys. Fluids **27**, 2139 (1984).
[17] H.Y. Guo et al., Phys. Plasmas **9**, 185 (2002).